

## Review

# Regenerative Medicine of Bone and Teeth

- with special references to biological principles, problems and their indicators -\*

Toshiyuki Kawakami<sup>1)</sup>, Yoshinori Kuboki<sup>2)</sup>, Junzo Tanaka<sup>3)</sup>, Shigeki Hijikata<sup>4)</sup>, Toshiyuki Akazawa<sup>5)</sup>, Masaru Murata<sup>6)</sup>, Ryuichi Fujisawa<sup>7)</sup>, Hiroko Takita<sup>7)</sup>, and Makoto Arisue<sup>6)</sup>

<sup>1)</sup> Matsumoto Dental University Graduate School of Oral Medicine, Shiojiri, 399-0781 Japan

<sup>2)</sup> Professor Emeritus, Hokkaido University, Sapporo, 060-8586 Japan

<sup>3)</sup> Tokyo Institute of Technology Graduate School of Science and Engineering, Tokyo, 152-8550 Japan

<sup>4)</sup> FGF Strategic Planning, Kaken Pharmaceutical Co., Ltd., Tokyo, 118-8650 Japan

<sup>5)</sup> Hokkaido Industrial Research Institute, Sapporo, 060-0819 Japan

<sup>6)</sup> Health Sciences University of Hokkaido School of Dentistry, Tobetsu, 061-0293 Japan

<sup>7)</sup> Hokkaido University Graduate School of Dental Medicine, Sapporo, 060-8586 Japan

(Accepted for publication, September 28, 2007)

**Abstract:** So much anticipation from the side of need patients has been caused by recent advances in tissue engineering technology. However, it seems that effective results can be hardly achieved unless we establish the proper principles for this technology. In this review paper, therefore, we discuss these problems and indicators from the viewpoint of the biological principles of hard tissue regeneration, which are as follows: 1) principles of hard tissue reconstruction, 2) bio-functional nano-composites for regeneration of hard tissue, 3) industrialization of growth factors for hard tissue reconstruction, 4) history and problems of medical ceramic materials, and 5) dentin matrices as a new autograft material for osseous regeneration.

key words: Bone, Tooth, Regenerative medicine

### 1) Principles of Hard Tissue Reconstruction

Aim of the session is to give a new insight into the mechanism of hard tissue formation, and thereby to reconsider the biological principles of tissue engineering. Any biocompatible substance, once if it is introduced into living tissues, is regarded as an “extracellular matrix (ECM)” by the cells there. It could be advocated from this idea that the term “biomaterials” is better referred to as “artificial ECM”, if we wish to emphasize the reaction of the material with cells and tissues. In this review on the principles of hard tissue reconstruction, we consider the artificial ECMs to be one of the major topics. Also, among the various properties of natural and artificial ECM, geometry is the most urgent area where we should focus our attention, because here we noticed that the knowledge in this area, so far, has not been elucidated systematically in spite of its practical importance. “Geometry” is defined principally as the structure of artificial

ECM at the micrometer level (roughly 0.1 - 1,000  $\mu$  m), and “ECM”, in this review, means in most cases artificial ECM.

### Five factors for tissue formation

We have proposed that five factors must be taken into

Five Factors of Tissue Formation

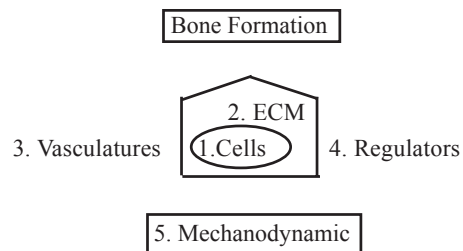


Figure 1. Five factors that influence tissue formation and reconstruction

\*The aim of the review is to provide a record of the “Biological Principles Required for Hard Tissue Reconstruction” symposium held during the 16th annual meeting of the Society for Hard Tissue Regenerative Biology, 2007.

Correspondence to: Dr. Toshiyuki Kawakami, Professor, Hard Tissue Pathology Unit, Matsumoto Dental University Graduate School of Oral Medicine, 1780 Hirooka-Gobara, Shijiri, 399-0781 Japan; Phone and Fax +81-263-51-2035; E-mail kawakami@po.mdu.ac.jp

consideration in order to understand the mechanisms of formation of hard tissues and to secure effective methods of reconstruction when they are partially defected or lost<sup>1-5)</sup>. These are [I] cells directly involved in bone formation, [II] natural and artificial extracellular matrices (ECM) produced by the cells, or “artificial

ECM”, [III] body fluids provided by vascularization, [IV] regulators of general cellular activities, and [V] biomechanical dynamics. (Figure 1) Lack of considerations on any one of factors may not lead to successful tissue reconstruction<sup>1-5</sup>.

These five factors should be analyzed individually; then the interactions between them can be elucidated; finally, they should be integrated into the whole picture of bone formation. These principles can be applied not only to understand the mechanism of bone formation but also to reconstruct local bone defects by tissue engineering. Usually, the actual application of two or three factors is enough for successful reconstruction of bone and related tissues. But care must always be taken to consider all other factors.

### ***Artificial ECM is a factor we can feasibly approach experimentally and then clinically***

One of the experimental systems to verify the above proposition is bone morphogenetic protein (BMP)-induced ectopic chondrogenesis and osteogenesis<sup>6-9</sup>. In this system, body fluid and some of the mechanical stress are already available in the local area if they are in the right place at the right time. The only items we must add usually are the regulators and the artificial ECM, which correspond to BMP and its carrier, respectively. BMP is a cytokine that was originally known for its unique ability to induce bone formation when it was implanted with a certain carrier into ectopic tissues such as skin or muscle<sup>6-7</sup>. This ability has naturally attracted the attention of scientists in the orthopedic and dental fields, including titanium implantology. One of the major problems to be overcome before clinical application is the development of the optimal carriers for this cytokine<sup>1-2</sup>. Thus, we have developed and tested more than ten different carriers<sup>1-5, 10-20, 22-25</sup>, including a new titanium device (titanium web)<sup>26-28</sup>. We have come to the conclusion that BMP-induced osteo- and chondrogenesis are highly dependent upon the nature of the carriers, notably upon their geometric properties<sup>1-5</sup>. This is partly because the carrier of BMP functions not only as a mere drug delivery system, but also as an important artificial ECM (cell substratum) on which the cells undergo growth and differentiation<sup>1-5</sup>. At the initial stage of research, BMP-induced bone formation was believed always to follow endochondral ossification<sup>7</sup>. However, when new carriers such as titanium web (TW)<sup>26-28</sup>,

porous particles of hydroxyapatite (HAP)<sup>13</sup> or fibrous collagen membrane (FCM)<sup>12, 14</sup> were introduced, it was found that bone could be formed directly following the process of membranous ossification, without any detectable amount of cartilage formation. Furthermore, nonporous particles of HAP did not induce any meaningful amounts of bone or cartilage under the same conditions<sup>13</sup>. A series of studies revealed that there are “vasculature-inducing carriers” such as porous particles or blocks of HAP<sup>16</sup> and “vasculature inhibiting (cartilage-inducing) carriers” such as fibrous glass membrane<sup>10, 25</sup>. These findings led us to investigate the detailed properties of natural and artificial ECM, particularly their geometrical properties.

### ***Taxonomy of properties and function of ECM***

Extracellular matrices have various properties and functions and they are categorized in many ways, but perhaps most fundamentally, they can be divided into [1] physical, [2] chemical, and [3] biochemical properties, and we have now come to a new phase where we have to add a fourth one, [4] geometry. Some of the examples of functions and properties are listed in Table 1. Among these properties, the physical, chemical and biochemical ones have been well studied and documented. However, geometrical properties of ECM have been poorly understood and studied only by a limited number of investigators.

(1) Physical Mechanical support for cells, tissues, organs and body (2) Chemical Support of cells and molecules through various chemical bonds supplying and depositing of various molecules (3) Biochemical Specific interactions among adhesion molecules, signaling molecules (cytokines) and cell surface receptors (4) Geometrical Directing growth and differentiation of cells and tissues

Geometry in this table is defined as the structure at the micrometer level (0.1~1000  $\mu$  m). Geometrical structures bigger than this range (macro-structure) are too large for cells to recognize. On the other hand the range smaller than this (nano-structure) is better discussed in relation to organic chemistry and structural biochemistry or, in modern terms “nano-biology”. Geometry of artificial ECM at the micrometer level is increasingly recognized for its importance in tissue engineering and regenerative medicine.

Table 1. Function and properties of natural and artificial ECM<sup>1,2)</sup>

Properties	Functions
(1) Physical	Mechanical support for cells, tissues, organs and body
(2) Chemical	Support of cells and molecules through various chemical bonds supplying and depositing of various molecules
(3) Biochemical	Specific interactions among adhesion molecules, signaling molecules (cytokines) and cell surface receptors
(4) Geometrical	Directing growth and differentiation of cells and tissues

Concerning titanium as an ECM, in Table 1 (four properties and functions), it is clearly shown that the distinguishing properties of titanium are its high physical strength and chemical stability. Moreover, once we give titanium products various geometrical structures, they are maintained for very long time in vivo, as well as in vitro culture situations. No artificial ECM other than titanium possesses this character.

any geometry of ECM and particularly when we design a new device with new geometry and specific functions. Before discussing the geometry of titanium as ECM in detail, it seems indispensable to investigate previous facts and meanings of the geometry of artificial ECM of any kinds. Thus, let us look back briefly into the history of artificial ECM based on geometries in Table 2.







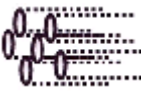



**Taxonomy of geometry artificial ECM**

In order to discuss the effects of geometry on cell activity and tissue formation, we attempted to classify the common geometries applied in artificial ECMs into ten categories, as shown in Table 2. It is thought that this classification is useful when we discuss

**Example of the studies in geometrical artificial ECM**

Numerous biomaterials (artificial ECM) have been devised and tested in pursuit of ideal materials as BMP carriers and other scaffolds for tissue regeneration in vivo or in vitro. During the process, a number of researchers have noticed that cells proliferate

Table 2. Ten categories of geometries found in artificial ECM at micrometer level (0.1-1000 μm). Modified from reference 2,4)

Groups	Categories <sup>1</sup>		Examples
Convex Groups	Fibers		Fibrous collagen membrane <sup>12,14)</sup> Fibrous glass membrane <sup>15,25,23)</sup> Titanium web <sup>26-28)</sup> CPSA glass fibers <sup>5)</sup>
	Particles		Insoluble bone matrix <sup>18,19)</sup> Porous particles of HAP with continuous pores <sup>16)</sup> Particles of HAP without pores Collagen beads <sup>22,23)</sup>
	Plane		Conventional culture dishes
Plane Groups	Sheet		Laser-perforated membrane <sup>17,20)</sup> (LPM,sheets with pores)
	Block		Porous blocks of hydroxyapatite <sup>16)</sup> ( HAP blocks with pores)
	Irregular pores		Porous particle of HAP <sup>10,11,13)</sup> Porous block of HAP <sup>16)</sup>
Concave Groups	Straight pores (Tunnels)		Honeycomb-shaped hydroxyapatite <sup>1-4)</sup> Honeycomb collagen Apatite-coateed honeycomb collagen <sup>22)</sup> Rat oncorisor tube <sup>28)</sup>
	Round concavities		Concavities on HAP monolith <sup>37)</sup>
	Rectangular concavities		Micro-pits on silicon tip <sup>38)</sup>
	Grooves		Microgrooves <sup>38,40)</sup>

and form tissues in different ways, when cells were placed upon the artificial ECM with the same substance but with different geometry<sup>1-5, 7, 10-27, 29</sup>. We will briefly follow some parts of the history of the studies in the geometry of artificial ECM.

#### ***Cartilage formation with close tube structure***

Reddi and Huggins were perhaps the first to notice the importance of the geometry of the ECM in cell differentiation and growth into tissues<sup>29</sup>. They constructed two geometrically different ECMs, a tube that was open at both ends and a dead-end tube, by cutting rat incisor dentin and implanting it into rat skin. After 4 weeks, they found that the open tube was filled with bone and marrow, while the dead-end tube was filled with cartilage.

The interpretation they made was that young mesenchymal cells (which the authors called fibroblasts at that time) in rat skin were induced to become chondrogenic and osteogenic cells by BMP that was contained in the decalcified dentin matrix. In the open tube, sufficient vascularization resulted in bone formation. But in the dead-end tube, particularly in the apical area, where vasculature and oxygen was scarce, young mesenchymal cells could not differentiate into bone and remained as chondrocytes, even at 100 days. Basset had already reported the phenomenon that the young mesenchymal cells were apt to form cartilage under oxygen-deficient circumstances, while they tended to differentiate into osteoblasts to form bone under oxygen-sufficient and mechanically-compressive conditions<sup>30</sup>. Also Folkman and Greenspan<sup>31</sup> commented that young cells can differentiate, according to a diffusion gradient, to oxygen and nutrients.

#### ***Sizes and shape of granular type ECM***

Reddi et al. also<sup>34</sup> reported the optimal size of granular ECM (decalcified bone powder) in BMP-induced bone formation to be around 420 – 850 $\mu$  m in particle size. With smaller particles (less than 74 $\mu$  m), cartilage and bone are scarcely formed<sup>34</sup>. The shape of granules is also important. Decalcified bone powders are usually irregular in shape and of porous structure, and in general are highly effective as a BMP carrier, but spherical HAP that not equipped with any porous structure is not effective as a BMP carrier<sup>13</sup>. Also, the size and shape of pores in the porous ECM are important determinant for tissue formation<sup>1-3, 16</sup>.

#### ***Vasculature-inhibiting geometry that leads chondrogenesis***

Inspired by the experiment done by Reddi and Huggis in 1997, we proposed that by providing artificial ECM, which inhibits vasculature ingrowth, but allows the young mesenchymal cells to enter and proliferate inside, we might arrest the chondrocyte stage in endochondral ossification. One of the reported artificial ECMs with such a microspace structure (vasculature-inhibiting geometry) was fibrous glass membrane (FGM)<sup>10, 15, 25</sup>, which was made of 1 $\mu$  m glass fibrils. Yoshimoto et al.<sup>33</sup> constructed a device, composed of a silicon tube (6 mm length and 3 mm internal

diameter) filled with FGM at a certain density together with 1 mg of recombinant human (rh)BMP-2, and implanted it into rat skin. They showed that this restricted system could maintain the cartilage stage of the endochondral process for a considerably longer period than the FGM without silicon tubing.

The results suggested that if a certain bioresorbable system of vasculature-inhibiting ECM is provided and implanted with BMP into skin or muscle, clinically auto-transplantable cartilage may be available. Following on from this work, Nawata et al.<sup>34</sup> enclosed the cultured mesenchymal cells with BMP in a diffusion chamber, which both inhibits vasculature and prevents new cells from entering, and implanted it into the abdominal subfascial pocket of a rat. After 5 weeks, they successfully obtained mature cartilage mass within the chamber, which upon reimplantation was able to repair full-thickness cartilage defect of the same strain of rat.

#### ***Vasculature and bone-inducing geometry***

Naturally, ECM with a permissible geometry for vasculature, can permit bone formation. Thus, vasculature-inducing geometry was proposed that promotes bone formation, in contrast to vasculature-inhibiting geometry, which promotes cartilage formation. It was found that porous particles of HAP (Table 2) that were equipped with interconnecting pores easily directed blood vessels throughout the pores of several different particles, when they were implanted into rats with BMP<sup>10, 11, 13</sup>. In the porous particles of HAP, the vasculature seems to run through neighboring particles, seeking out the orifices of pores that are oriented in the same direction in adjacent particles, just as tree roots develop, finding spaces inside rocks. Vasculature development needs appropriate spaces. This is a reason why interconnected pores are indispensable in ECMs for bone reconstruction. “Vasculature-inducing geometry” and “vasculature-inhibiting geometry” are fundamentally important concepts in ECM geometry. These concepts not only create bone and cartilage differentially, but also may open a strategy for tissue engineering. Next, let us consider vasculature-inducing geometry in more details.

#### ***The optimal pore size for bone formation is nearly that of the Havarsian system***

Tsuruga et al.<sup>16</sup> compared bone-inducing efficacies of five different porous blocks of HAP, having pore sizes of 106-212, 212-300, 300-400, 400-500, and 500-600 $\mu$  m, respectively. A block (approximately 5 x 5 x 1 mm, 40 mg) of each HAP ceramic was combined with 4 $\mu$  g of rhBMP-2 and implanted into the back skin of a rat. Bone-inductive ability was estimated by alkaline phosphatase activity at 2 weeks and osteocalcin contents at 4 weeks after implantation. Results revealed that the highest amount of bone was produced in the ceramics with a pore size of 300-400  $\mu$  m.

Interestingly, histological observation of osteogenesis within the pores showed that the bone formed concentrically along the

inner walls of the pores, whose sizes were from 100 to 500  $\mu$  m. However, within the pores of 500-600  $\mu$  m, bone did not form concentrically along the inner wall of pores but developed irregularly inside the pores. The results indicated that osteoblasts could recognize the curvature geometry of round-shaped pores up to 400-500  $\mu$  m in diameter, and construct the concentric bone along the inner wall of pores. However, osteoblasts could no longer recognize the larger curvatures above 500  $\mu$  m in diameter, and could not form concentric layers along the surface of the pores in this HAP material. It was tentatively concluded from these experiments that the critical diameter of curvature that osteoblasts can recognize is approximately 500 $\mu$  m (250  $\mu$  m in radius). Normal bone is always remodeling in a concentric manner to form Haversian systems. It is not surprising that the optimal size of pores in artificial ECM coincides with the average diameter of the Haversian system that is 200-300  $\mu$  m. However, if we use the ECM other than pure HAP ceramics, there is a possibility that osteoblasts may behave in a somewhat different way.

#### **Tissue formation within the honeycomb-type straight tunnels**

As discussed above, the inner wall of a tubing structure of interconnecting pores of 300-400 $\mu$  m in diameter will provide the ideal geometrical environment for osteogenesis. One of the explanations of this phenomenon is that such geometry will generate a higher cell density than a convex or flat surface as shown in Figure 2. However, most of the porous ceramics so far proposed to have “interconnected” pores are, in fact, equipped

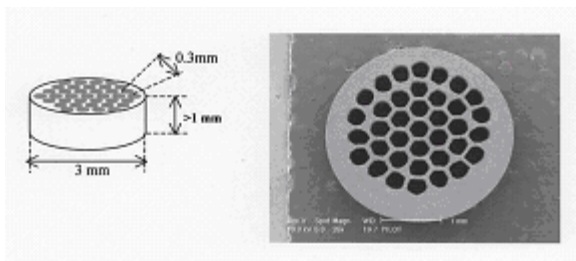


Figure 2. An example of three-dimensional (3D) geometric artificial ECM of honeycomb-shaped ceramics with 37 tunnels made of  $\beta$ -tricalcium phosphate (Pilot Precision Co., Japan). In this bio-resorbable artificial ECM, the number and size of the tunnels are strictly controllable in the production process. The length of the ECM can be varied from 1-10 cm. Various cells and tissues can enter into the tunnels and develop in specific ways, dependent upon their characteristics.

with irregular pores, not straight tunnels. It was expected that honeycomb-type straight tunnels would more directly exert the geometrical effect upon the growth of bone and other tissues than irregular “interconnected” pores. Inspired by this idea we have developed honeycomb-shaped geometrical ECM made of ceramics, in collaboration with Hokkaido University and Pilot Precision Co., Japan <sup>1-5)</sup>

The effect of tunnel size upon bone and cartilage formation

was clearly shown when we compared the tissue formations between two different honeycomb apatite ceramics, those with smaller (90-110  $\mu$  m) and larger tunnels (350 $\mu$  m) <sup>1)</sup>.

The explanation of the results is as follows: in the smaller tunnels, young mesenchymal cells can enter from the beginning, but vasculature takes time to develop in the tunnel. This situation leads to chondrogenesis and can fill the tunnels with cartilage at 2 weeks. With time, vasculature develops in the tunnels and the cartilage is gradually replaced by bone from both orifices. At 4 weeks, concentric bone fills the tunnel as vasculature runs through. In the larger 350  $\mu$  m tunnels, condensation of mesenchymal cells was accompanied by vasculature at 1 week, which leads situation led to direct bone formation without any detectable cartilage formation throughout the experimental period. These results clearly indicate that the honeycomb-type geometry with straight tunnels could enhance or inhibit a certain process of tissue formation, as was shown in the examples of direct bone formation and endochondral ossification in this particular experiment.

There are several examples of honeycomb-shaped ECM, other than those made of calcium phosphate ceramics, which direct or control tissue formations. Those include a honeycomb-type insoluble collagen (Collagen Sponge Honeycomb, Koken Co., Tokyo) <sup>21, 22, 35)</sup>, a laser-perforated polymer membrane (LPM) of bio-degradable properties<sup>17, 20)</sup>, and honeycomb-shaped polymer films<sup>36)</sup>. It was already shown that a honeycomb-type insoluble collagen promoted the differentiation of mesenchymal stem cells into osteoblasts<sup>35)</sup>, directed Haversian system formation<sup>22)</sup>, and promoted growth of peripheral nerve fibers <sup>22)</sup>. It was reported that the LPM directed collagen fibril formation<sup>17, 20)</sup>, and honeycomb film guided differentiation and growth of nerve stem cells<sup>36)</sup>.

#### **Concave geometry and optimal space theory**

In Table 2, we have divided all of the geometries of ECM into three large groups: convex, plane and concave. So far, we concentrated the discussion on concave group and have concluded from the numerous previous examples that as far as bone formation is concerned, concave geometry of ECM is advantageous over convex or flat. The possible mechanisms involved are as follows: (1) concave geometry permits a higher concentration of cells, (2) it leads to effective accumulation of cytokine and other active bio-molecules (3), there is a closer chance of cell-cell communication and (4) the creation of three-dimensional (3D) environments occurs more quickly than does those of two-dimensional (2D). The optimal diameter of pores or tunnel structures was concluded to be 300-400  $\mu$  m, and the effective radius of curvature up to about 250  $\mu$  m, as shown in the preceding discussion. These conclusions concerning the size of concave geometry are not only applicable to completed pores or tunnels, but also may be partially eligible to open pore structures (concavities), rectangular concavities<sup>38)</sup> and grooves<sup>39, 40)</sup>, as shown

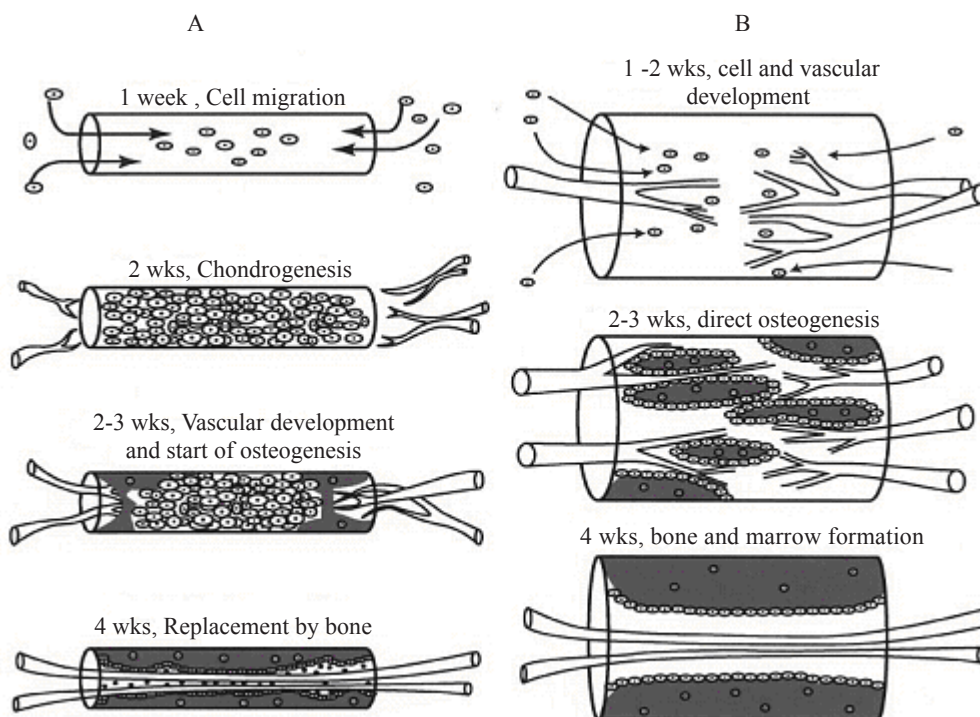


Figure 3 shows a schematic representation of geometry-directed chondrogenesis and osteogenesis in the honeycomb HAP (HCHAP) with smaller (A) and larger (B) tunnels, which were applied as BMP carriers. In the smaller tunnels (90-110  $\mu\text{m}$  in diameter), cartilage was formed followed by bone formation, similar to the process of endochondral ossification. Contrastingly, in the larger tunnels (350  $\mu\text{m}$  in diameter), bone was formed directly without detectable cartilage formation.

in Table 2. Hirano et al. created a tartan-patterned grooved surface with 500  $\mu\text{m}$  wide grooves on titanium alloy rod. These grooves promoted faster bone ingrowth, resulting in a stronger bond with bone when implanted into the rabbit femoral condyle<sup>40</sup>.

When we look at histology in many studies on BMP-induced bone formation, we find generally that most of the initial bone formation started at the concave area of ECM<sup>12</sup>. Furthermore, even without the addition of BMP or cytokines, several authors have reported that osteogenesis were observed in concavities and pores of ceramics in vivo. Ripamoti and coworkers found osteogenesis in the concavities of HAP ceramics, which were implanted into baboon muscles without BMP<sup>37</sup>. Endo et al. also reported bone formation in porous  $\beta\text{TCP}$  ceramics (porosity of 75%, pore size 100-500  $\mu\text{m}$ ) implanted in the muscle of beagle dogs, 56 days after implantation without BMP<sup>41</sup>. Again it should be noted that initial bone formation occurred in the concave part of the ceramics in both studies.

Proposal of “optimal space theory”: these observations led us to the concept of “optimal spaces for tissue formation in artificial ECM”. By this concept we propose that each kind of tissue ECMs has an optimal geometrical shape and size, which facilitate its cells to differentiate, proliferate and develop particular tissue in a certain direction. These optimal spaces are not limited to tube- or sphere-types, but include certain spaces between the solid ECM

structures, such as fibers, particles, and flat planes as shown in Table 2. The size of the optimal spaces is assumed to be approximately 200-500 $\mu\text{m}$  which is dependent upon tissues.

#### ***Titanium web as an example of fiber-type ECM***

The fibrous ECMs, which are classified as convex-groups in Table 2, can also compose optimal 3D spaces. However, the spaces are distorted and often collapse when the fibrous ECMs are implanted into the body. Conventional examples are fibrous membranes of polylactic acid and its copolymer with polycaprolactone, and cross-linked collagen fibrous membranes. In this regard, the titanium web (TW) construct is an extremely rigid fibrous structure<sup>26-28</sup>. The 3D structure of TW is composed of thin titanium fibers 50-100  $\mu\text{m}$  in diameter. The cross section of the fibers in this material is not round but square, due to its manufacturing process. Each titanium fiber is fused to adjacent ones by vacuum sintering, so that the network or web structure is strong and can be molded into any form indicating, disks (Figure 4 and B), blocks (Figure 4 C), or even tubing. The disk form of the titanium web has been applied to 3D cultures of osteoblasts and mesenchymal stem cells (Figure 4A, B, C and D)<sup>42</sup>. The results indicated that TW as 3D culture system generally increased cell proliferation due to its large surface area, and promoted differentiation due to its 3D effects on the cells, compared with

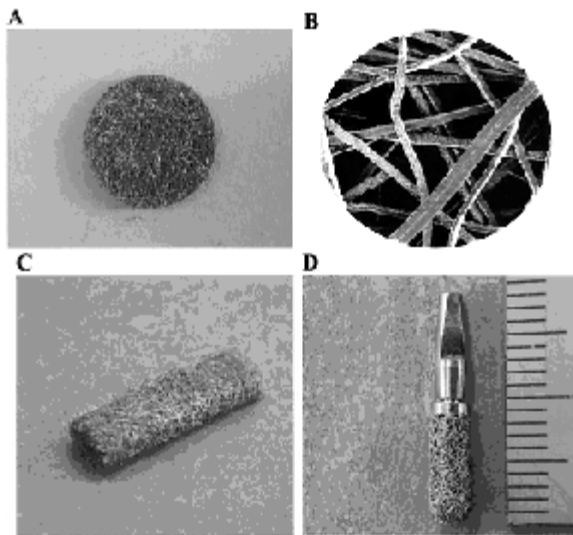


Figure 4. Various three-dimensional products made of titanium web (TW): TW-disk (A, B), TW-block of 3 x 6 x 25 mm (C), and TW-equipped titanium rod (TWT), a tooth model (D). In TW-disk (A), titanium fibers (50  $\mu$ m in diameter) are sintered into disk form 1.5 x 15 mm for use in 3D culture. The Scanning Electron Microscope-image of the TW-disk is shown in B; fibers of rectangular shape are clearly recognized. In TWT, a tooth implant model, TW was vacuum sintered onto the cylindrical root implant made of titanium, to the upper part of which an abutment was attached (Products from Hi-Lex Corporation, Japan).

conventional cultures on a flat dish<sup>42</sup>). There are increasing needs for appropriate ECMs for 3D culture systems. Day by day we need more information on cell behavior in a 3D environment, in addition to the 2D environments of conventional flat culture dishes<sup>43, 44</sup>).

We should recall that five factors are required for tissue reconstruction, as discussed in the beginning. If we provide the cells with appropriate houses (matrices), nutrition (vasculature) and some of the stimulations (regulators and biomechanical dynamics), they will build up tissues and organs.

## 2) Bio-Functional Nano-Composites for Regeneration of Hard Tissue

Biological tissues have peculiar structures organized on a nanometer-scale. In order to synthesize such biomimetic nanostructure materials or novel functional biomaterials, interfacial interactions between constituents are important. In this section, two examples of bio-functional nano-composites are introduced for the application of clinical treatments such as osteoporosis and metastatic bony carcinoma.

Tissue engineering includes the following biological processes: (1) proliferation of functional cells mainly derived from patients themselves; (2) formation of cell-based constructs with sufficient size *in vitro*; (3) implantation of the constructs to the defects; and (4) regeneration of tissue *in vivo*. In general, bioaffinitive materials, i.e. scaffolds, are necessary to make useful cell-based constructs.

For hard tissue regeneration, possible scaffolds are ceramics, as well as bioabsorbable polymers and/or their composites. Ohgushi et al. confirmed heterotopic ossification by the implantation of osteoblasts on porous ceramics including HAp<sup>45-47</sup>), and applied this technique to human knee joint replacement<sup>48</sup>). In bone remodeling metabolism, scaffolds are required to have an appropriate decomposition rate; therefore, the size of HAp crystals and the state of collagen fibrillogenesis in the scaffolds should be similar to those in bone. It is therefore expected that the decomposition of such HAp/Col composite should show the same reaction as autologous transplanted to a bone defect, depending on osteoclasts.

### Biomimetic synthesis of bone-like nanocomposite

In osteogenesis, osteoblasts provide raw materials, mainly collagen and HAp (calcium phosphate), which are spontaneously aligned to the nano-ordered structure of bone<sup>49</sup>). In bone formation, osteoblasts appear to control a self-organization process of

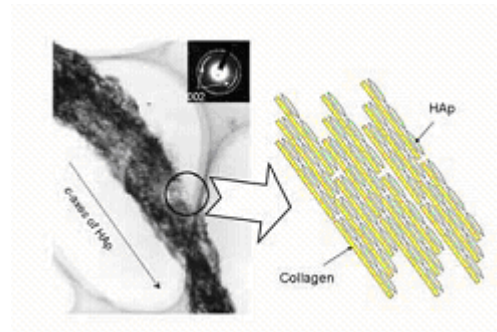


Figure 5. Transmission electron microscopic image of a HAp/Col composite, and self-organized nano- structure

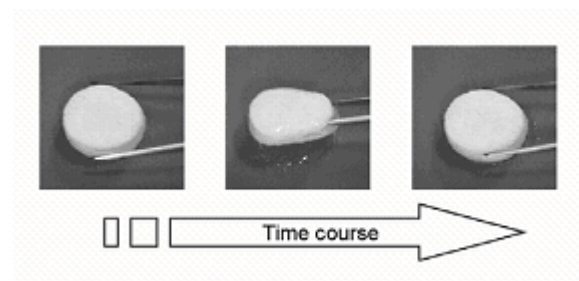


Figure 6. Sponge-like porous HAp/Col composite.

collagen and HAp as a chemical reaction. Therefore, the HAp/Col nanocomposite with similar chemical composition and nanostructure to bone should be synthesized on the basis of the self-organization mechanism of bone<sup>50-53</sup>). The HAp/Col composite has a good cell attachment property.

The starting materials for HAp/Col composite are  $\text{Ca}(\text{OH})_2$ ,  $\text{H}_3\text{PO}_4$  and collagen. In our studies, we have used  $\text{Ca}(\text{OH})_2$  prepared from  $\text{CaCO}_3$  (alkaline analysis grade, Wako Pure Chemicals Inc.). HAp stably forms under weak basic pH 9. The collagen we

used was atelocollagen extracted from porcine dermis (biomaterial grade, Nitta Gelatin Inc.): its isoelectric point was pH 7-9.

Self-organization of HAp and collagen are promoted at 40 °C and pH 8-9. This pH value is larger than that of animal body fluid, normally pH 7.2 to 7.4, indicating that bone forms also under such pH conditions controlled by osteoblasts. Fibrillogenesis of collagen is promoted around 40 °C and under ion strength similar to body fluid. The TEM image of the composite obtained is shown in Figure 5, together with its schematic nanostructure. The maximal length of the HAp/Col self-organized fiber was 75  $\mu$  m in length; the longest fiber was synthesized in a reaction vessel with ion concentration less than 1/700 of PBS.

Dense bodies of the HAp/Col composite were obtained by filtration and dehydration of fibers under high pressure, as the HAp/Col fibers contain a large amount of water. Further, porous bodies of the HAp/Col self-organized composites were prepared from fibers by a freeze-dry method. The HAp/Col porous body demonstrated sponge-like viscoelastic property as shown in Figure 6, which increases cell migration.

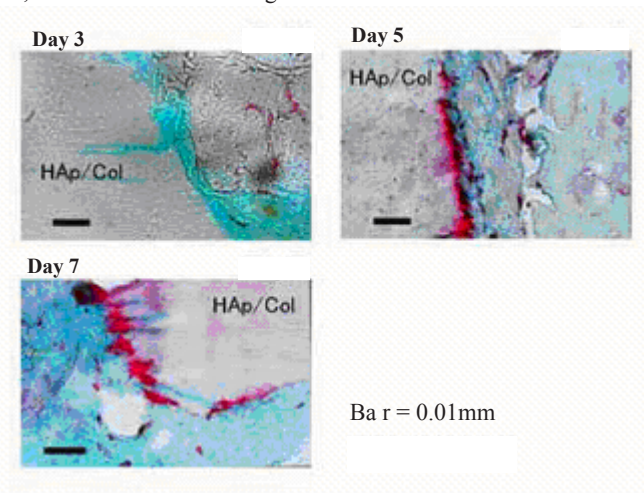


Figure 7. Histochemical TRAP stained section of the HAp/Col composite implanted into rat tibia.

#### Biological reaction of the HAp/Col composite

The HAp/Col composites were implanted in bone, and the biological reaction was examined. Figure 7 shows the HAp/Col composite implanted into a rat tibia for 5 days, stained with histochemical tartrate resistant acid phosphatase (TRAP). TRAP active multinuclear giant cells were identified as osteoclasts, which were observed onto the HAp/Col surface. The porous HAp/Col composite was finally substituted to bone by the remodeling metabolism.

After the appearance of osteoblasts, alkaline phosphatase (AIP) positive cells were induced in the neighborhood of osteoclasts around the HAp/Col composite as shown in Figure 8, and were identified as osteoblasts that form bone. This reaction continues until the HAp/Col nanocomposite was completely absorbed, and

finally the HAp/Col nanocomposites were substituted to new bone<sup>50,52,53</sup>. The absorption of the composite and the bone formation reaction was almost the same reaction as in/for autografted bone. This result suggests that the HAp/Col nanocomposite was recognized as “bone” by bone tissue and was incorporated into bone remodeling metabolism.

The HAp/Col porous bodies with sponge-like viscoelasticity were implanted into bone defects with appropriate deformation. The viscoelastic property was very suitable for a bone-filler and for tissue engineering of hard tissue, as it is difficult to seed cells in a 3-dimensional scaffold homogeneously. The HAp/Col porous body allowed homogeneous cell migration by repeatedly deforming the sample in a cell suspension. The porous structure of the HAp/Col composite was well-maintained after the deformation, much better than a pure collagen sponge and other biodegradable polymers even after medium exchange infiltration.

#### Nano-crystals for DDS of bony metastatic cancer

Recently a drug delivery system (DDS) has been studied from material-scientific points of view to improve the efficiency of drugs and/or reduce their side effects. In order to develop a DDS for the treatment of metastatic bony carcinoma, a calcium phosphate system, such as HAp and octacalcium phosphate (OCP), was adopted as a DDS carrier. Bisphosphonate Bps, such as etidronate, was controlled to into the nano-particles of HAp and OCP. It is thought that OCP forms an intercalation compound, prepared by a wet method in the presence of bisphosphonate. As shown in Figure 8, such a compound could automatically control the activity of osteoclasts, useful for the treatment of metastatic bony carcinoma.

Nano-composites such as HAp/Col and OCP/drug are responsible for osteoclasts. It was shown that this osteoclast-responsibility could be applied to new bone formation and automatic control of osteoclast activity.

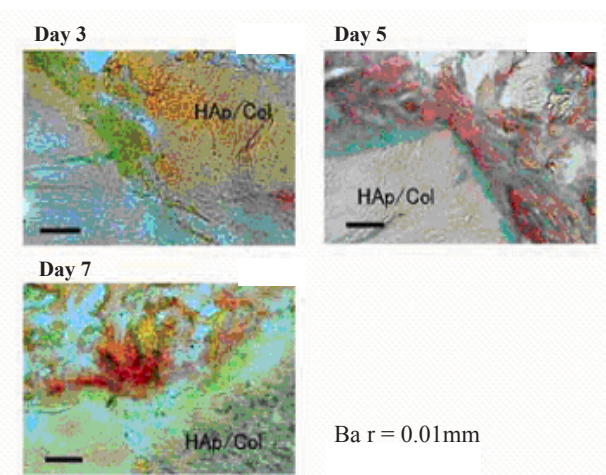


Figure 8. The HAp/Col composite implanted into a rat tibia; stained by histochemical AIP.



**3) Industrialization of Growth Factors for Hard Tissue Regeneration**

In Japan, neither medical drugs nor medical devices for the reconstruction of hard tissue regeneration have been sold, while those which have been launched in USA and Europe and have contributed to cure of disease. The components in these medical products originally exist in the body and have properties to

Ross et al. discovered Platelet-Derived Growth Factor (PDGF) as the causal factor of arterial sclerosis. In 1965, Urist discovered a factor that induces osteogenesis<sup>6)</sup> and named it Bone Morphogenic Protein (BMP). Subsequent studies demonstrate that BMP belongs to TGF-  $\beta$  super family. Nakamura et al. discovered Hepatocyte Growth Factor (HGF) in 1984 as the growth factor of hepatocytes<sup>59)</sup>. At present attention is on as the

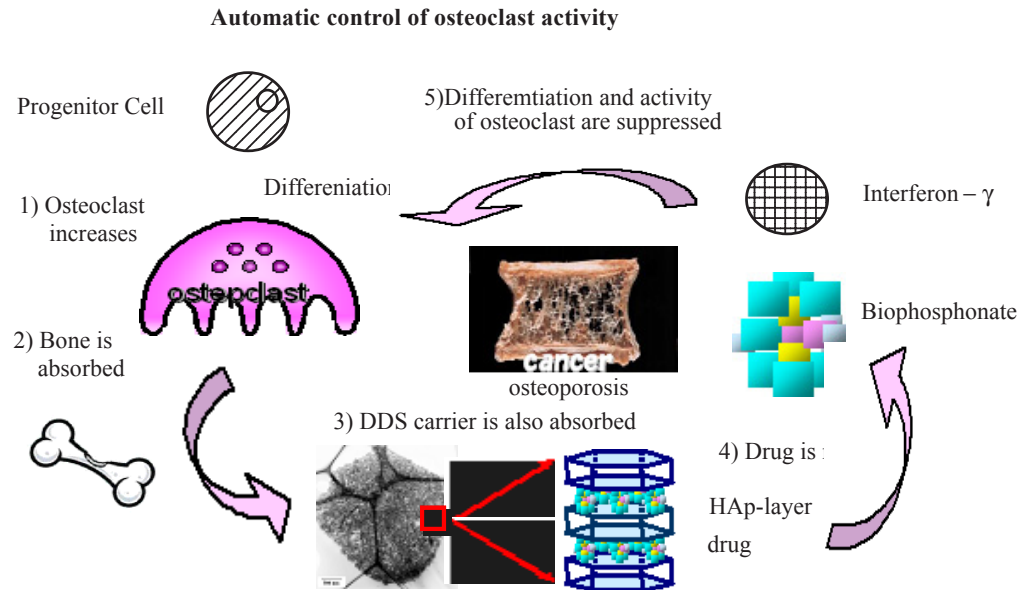


Figure 9. Concept for development of new DDS carrier of metastatic bony cancer.

accelerate the proliferation or the differentiation of a cell. With the development of genetic technology, mass-production of these substances became possible. We have expected the application of these substances to the regeneration of skin, cornea, blood vessel, etc. as well as osteogenesis, and some substances have been used for medical purpose. In this section, we will describe the discovery history of these main factors and the situation of their industrialization.

**Discovery history of cell growth factors**

Cell growth factors were first discovered in the 1950s. The Levi-Montalcini group found Nerve Growth Factor (NGF) as the substance that is involved in the survival and growth of nerve cells<sup>54)</sup>. Levi-Montalcini received a Nobel Prize in 1986 together with Cohen<sup>55)</sup>, who discovered Epidermal Growth Factor (EGF) in 1962. In 1974, Fibroblast Growth factor (FGF) was found by Gospodarowicz as the factor to accelerate the proliferation of 3T3 cell lines that were extracted from the bovine pituitary gland<sup>56)</sup>. Subsequent studies confirm that this FGF stimulates the proliferation of vascular endothelial cells, smooth muscle cells, cartilage cells, and mesenchymal stem cells. In 1984, the existence of basic Fibroblast Growth Factor (bFGF, FGF-2) and acidic Fibroblast Growth Factor ( $\alpha$ FGF, FGF-1) was demonstrated<sup>57,58)</sup>.

angiogenic factor. Vascular Endothelial Growth Factor (VEGF) is a strong growth factor for vascular endothelial cells, and in 1989 a group by Ferrara discovered it<sup>60)</sup>. Studies thereafter have clearly indicated that VEGF is the same as Vascular Permeability Factor (VPF) found in 1983<sup>61)</sup>.

**Situation of industrialization of products for hard tissue regeneration**

BMP-2 has already been launched in the US and European countries as the alternative material for bone graft in combination with collagen sponge. It has been used to meet the three indications of acceleration of spinal fusion, open tibia fracture, and the regeneration of alveolar and mandibular bone. The US is the first country in which the product was launched in 2002, followed by Europe in 2005. The product name is INFUSE<sup>®</sup> Bonegraft in the US and InductOS<sup>®</sup> in Europe.

In Japan, Yamanouchi Pharmaceuticals Co., Ltd. (now Astellas Pharma Inc.) completed clinical studies for spinal fusion and applied for manufacturing approval. It has not yet been approved, and development rights and distributorship were sold to Medtronic Japan Co., Ltd. Similarly to BMP-2, OP-1 was developed as the adjuvant therapy for spinal fusion and long bones. It has already been launched in the US, Europe, Australia, and Canada, under

the product name OP-1®. In combination with βTCP, PDGF has already been launched in the US as the medical device to repair the defect of alveolar bone due to periodontal disease. Under the product name GEM21S®. In addition, PGDF has already been sold under the name Regranex®gel in the US, Europe, Canada, Korea, etc., as a medicine for diabetic skin ulcers. In 1986, Abraham's group in California Biotechnology Inc., USA (now Scios Inc.) reported that the group clarified the DNA sequence of human bFGF<sup>62</sup>. Kaken Pharmaceutical Co., Ltd. contracted with Scios Inc. in 1988 and began its development in Japan. It was launched under the trade name Fiblast®Spray (Figure 10) in 2001, and the indications for bedsors and skin ulcers (burn ulcers/leg ulcers). Clinical trials of bFGF are ongoing in Japan as a drug for bone fractures and the regeneration of periodontal tissues.

**Issues in the development of drugs for hard tissue regeneration**

Cell growth factors that have been expected as the drugs for the regeneration of hard tissues are proteins. They are unstable materials and structural changes easily occur. This instability is a large barrier to the development of protein formulations. In-depth stabilization technology based on physicochemical studies and analysis techniques with high quality for support are required in



Figure 10. Fiblast® spray

order to overcome these issues.

When bFGF or PDGF were intravenously administered to rats, these accumulate in the liver and kidney<sup>63,64</sup>. When bFGF was subcutaneously dosed to rats for 3 months repeatedly, the excretion of urinary proteins markedly increased<sup>65</sup>. The intravenous administration of bFGF clinically caused hypotension<sup>66</sup> and an increase in urinary proteins<sup>67</sup>. On the other hand, studies on local application of bFGF confirmed no transfer of bFGF to the blood<sup>68</sup>. In addition, it is well known that growth factors are involved in the acceleration of growth of tumor cells. Therefore, we believe that the systemic administration of growth factors should be avoided as much as possible for safety.

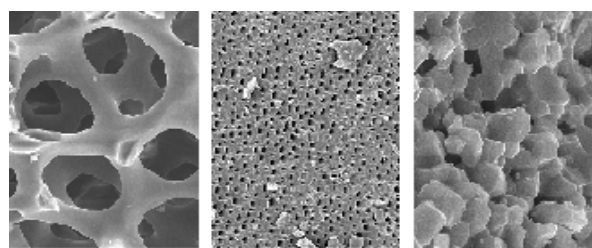
**4) Development of bioabsorbable and biomimetic ceramics and A big prospect for regenerative therapy-studies in Hokkaido**

In graving society, for regenerative therapy for patients,

ceramics in medicine are important biomaterials and collaboration among the educational-industrial-administrative complex is an effective action. After returning the transition of bioceramics, functionally graded apatites (fg-HAp) originated from natural bone will be outlined as an interdisciplinary study focusing on biomimetic materials. The role and scheme of regenerative therapy-studies that are useful out there will be discussed. Since fg-HAp has excellent degradation-absorption, rhBMP-2-adsorption and release characteristics due to body fluid permeation and blood permeability, rhBMP-2/fg-HAp is an osteoinductive bioceramic with bone-remodeling. The fg-HAp can be designed and controlled by the calcination and dissolution-precipitation and it might be applied to higher advanced medical care by strong connection with medical and dental teams.

**Biomimetic materials and collaborate study in an interdisciplinary field biomimetic ceramics for regenerative therapy**

Figure 11 shows SEM photographs of three living tissues-originated materials. For starfish, calcium carbonate (CaCO<sub>3</sub>) ceramics with homogeneous pore diameters of about 10μm were obtained by the decomposition by enzymes and the calcination at 600°C for 2h in air. For dentin from extracted teeth, a lot of dentinal tubules with 1-2 μm were observed. For bovine bone, hexagonal grains in 1-2 μm with single phase of hydroxyapatite (HAp) were designed by the calcination at 1100°C for 24h in air. Living tissues-originated materials contain the grain morphology, the surface structure, and the chemical nature which originate from small amounts of metal ions in a living environment<sup>69</sup>. Biomimetic ceramics are functional materials that are efficient for maintaining optimal environment for cells or biopolymers. We focused on the development of degradable and bioabsorbable HAp, which can be used as chief biomimetic ceramics for regenerative therapy.



a) Starfish                      b) Dentin                      c) Bovine bone

Figure 11. SEM photographs of living tissues-originated materials

**Regenerative therapy-studies recognized by the Hokkaido government through collaboration among the industrial-educational-administrative complex**

In bone reconstruction or regenerative therapy, development and application of artificial organs imitating living tissues, medical devices, and medical systems, have been expected. Research and

development of biomaterials should be carried out by the fusion of many techniques, such as medical research, biotechnology, and materials engineering. Figure 12 shows collaborative studies on biomaterials and regenerative therapy in an interdisciplinary field. The title of the study is “Development of functional biomaterials

satisfactory materials for bone regeneration and long-time use. Coping with various needs of patients, i.e. implanting location or situation, development of tailored HAp ceramics which can strike a reasonable balance between bioabsorption rate and mechanical strength in a living body have been expected<sup>8)</sup>. The tailored

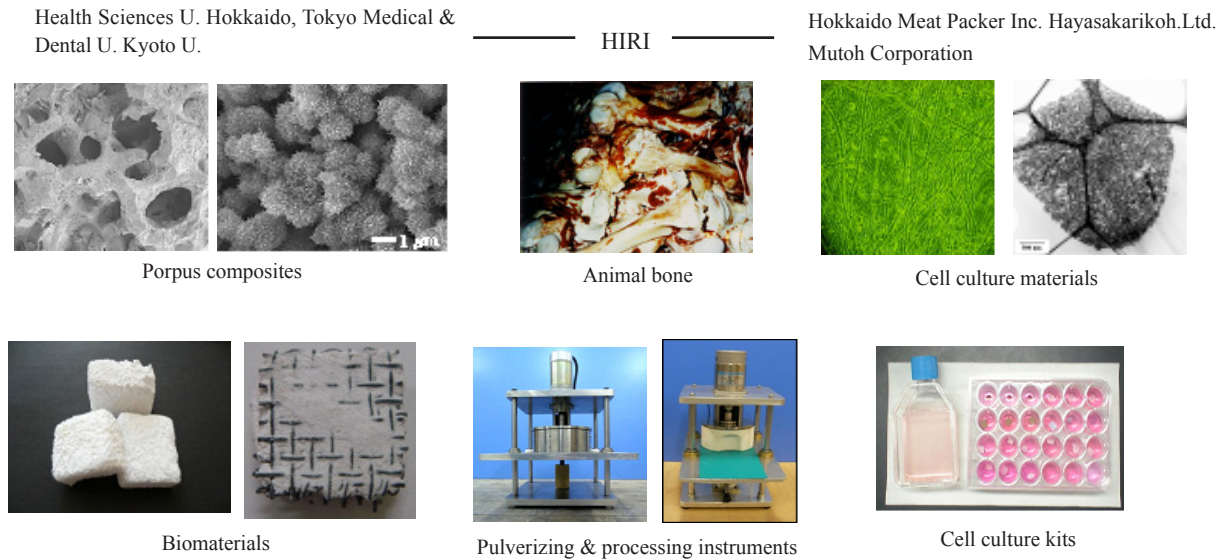


Figure 12. Collaborate studies on biomaterials and regenerative therapy in an interdisciplinary field

and their application for regenerative therapy and advanced medical engineering”, performed as a special study in Hokkaido by seven agencies in 2006-2008. Hokkaido Industrial Research Institute (HIRI) built up a big project team, which consists of Kyoto University, Tokyo Medical and Dental University, Health Sciences University of Hokkaido and three companies. The three universities have high basic technology on biomaterials and cell engineering and the three companies possess the know-how and facilities for production and sale of medical equipment and safe treatment of animal bone. For the purpose promoting a bio-industry cluster in Hokkaido and utilizing Hokkaido resources, through the fusion of bioscience and nanotechnology, we are preparing porous composites using animal bone and developing cell culture kits or pulverizing and processing instruments to apply for regenerative therapy and advanced medical engineering.

***Invention of bioabsorbable and functionally graded apatites  
Development of tailored ceramics***

For bone reconstruction and bone regeneration, many kinds of biomaterials have been developed<sup>70-74)</sup>. Hydroxyapatite (HAp) and  $\beta$ -TCP can be applied as bioactive and substituted materials for hard tissues in the dental and medical fields because of excellent biocompatibility and osteoconduction<sup>75)</sup>. However, HAp ceramics synthesized from reagents show very low bioabsorption characteristics in implanted regions even after several years. Therefore, commercial HAp ceramics cannot always be

ceramics would be absorbed and substituted for mother tissues after operation, depending on the new bone formation and bone regeneration. We arranged the required capability of apatite products for the biomaterials early incorporated into bio-metabolic system. The new apatite products need to be bioceramics with excellent body fluid permeability, high surface area, appropriate mechanical strength, and high activity for various cells. Responding to the necessary conditions, functionally graded and porous ceramics, in which grain size and crystallinity of HAp gradually change from surface region to bulk part, were considered. We tried to control absorption and osteoinduction characteristics by loading of recombinant human bone morphogenetic protein-2 (rhBMP-2) into the ceramics.

***Biomimetic ceramics prepared using animal bone***

Safe animal bone was supplied from traceable livestock in Hokkaido Meat Packer Incorporation. To design biomimetic materials originated from animal bone, recycle techniques of apatite resources and dissolution-precipitation conditions in ceramics engineering were discussed. Bioabsorbable ceramics with spongy bone-originated skeleton structure and pore structure of nano-particles, which may promote body fluid permeability and cells-affinity, were prepared.

***Design of fg-HAp ceramics derived from bovine bone***

Spongy and cortical bovine femur bones were used as starting

materials, boiled and calcined at 800-1100°C for 24h in air to obtain crystalline HAp (b-HAp) ceramics. By the calcination process, all prion proteins and organic residues of bovine bone were completely burned out. The pulverized cortical b-HAp was completely dissolved into a HNO<sub>3</sub> solution, while the spongy b-HAp was partially dissolved into another HNO<sub>3</sub> solution. After the solutions were mixed, NH<sub>3</sub> solution was added and reprecipitated HAp (r-HAp) crystals were carefully precipitated on macro-pores and micro-pores of spongy b-HAp at pH 10.5 and 25°C<sup>5)</sup>. The modified spongy b-HAp was aged for 24 h to fabricate a structure of fg-HAp. The fg-HAp ceramics were filtrated and washed with distilled water and dried at 120°C. To obtain rhBMP-2/fg-HAp ceramics, rhBMP-2 (5µg) solution was added to fg-HAp ceramics in a sterilized dish.

#### *Microstructure and crystallinity of biomimetic fg-HAp ceramics*

fg-HAp had same chemical composition as b-HAp and r-HAp<sup>77-79)</sup>. The (Ca/P) ratios of fg-HAp were 1.64-1.66, which are close to the stoichiometric value of 1.67 for the standard HAp. Small amounts of Na<sup>+</sup> and Mg<sup>2+</sup> ions, present at less than 1%, were detected. The fg-HAp ceramics exhibited mechanical strengths sufficient for operation and handling of animal experiments. Figure 13 shows the appearance and SEM photographs of fg-HAp ceramics prepared by the calcination at 800°C and partial dissolution-precipitation. Spherical moss-like grains forming needle-like microcrystals and macro-pore sizes of 100-800 µm were observed. The specific surface areas, total pore volumes, and porosities of the ceramics were 30-40 m<sup>2</sup>.g<sup>-1</sup>, 0.35-0.40 cm<sup>3</sup>.g<sup>-1</sup>, and 60-80 %, respectively. In the curves of the pore size distribution for the ceramics, pore volumes in the micro-pore sizes of 10-160 nm were clearly recognized. The Micro-XRD analyses indicated that the degree of crystallinity of the single phase HAp was gradually distributed from the surface layer of the macro-pore wall to the bulk region of the b-HAp body structure.

Based on these results, it was found that the pore structure of the fg-HAp was classified into a macro-pore (100-800 µm) originating from spongy bone and a micro-pore (10-160 nm) prepared by the calcination and partial dissolution-precipitation<sup>78)</sup>. The fg-HAp ceramics with the specified pore structures and

gradations in both crystallinity and grain size can permit body fluid to easily permeate the parts of a living body. Also, microcracks in bulk regions of the ceramics formed by partial dissolution with HNO<sub>3</sub> may be related to auto-degradation and body fluid permeation. Moreover, the fg-HAp ceramics were certificated to be abnormal prion-free materials by the enzyme antibody reaction kit (Bio-Rad) for diagnosing bovine spongiform encephalopathy in Obihiro University of Agricultural and Veterinary Medicine.

#### *Characterization of biocompatibility for different HAp ceramics by soaking in SBF*

For evaluation biocompatibility of the ceramics, each of the fg-HAp and b-HAp ceramics was soaked at 36.5°C and pH 7.4 in a simulated body fluid (SBF) for 1-90 days<sup>79)</sup>. The SBF is the solution which ion concentrations and pH nearly equal to those in human plasma at 36.5°C. Figures 14 shows photographs of the b-HAp and fg-HAp ceramics soaked at 36.5 K and pH 7.4 in SBF for 1, 8, 14, and 28 days. The b-HAp was calcined at 800°C for 24 h in air. At 14 days after the soaking, microstructure of the b-HAp became porous urchin-like grains of 5-6 µm, while at 8 days, that of the fg-HAp already changed from small grains to dense cocoon-like ones by rapid precipitation of HAp microcrystals. These significant differences in surface morphology suggest that the fg-HAp has higher bone-bonding ability than the b-HAp, and that, concerning proteins-adsorption on the two ceramics surfaces, the fg-HAp surfaces show larger amounts of proteins adsorbed and higher adsorption heats for proteins because r-HAp microcrystals on the sintered grains enhance surface roughness of the b-HAp ceramics.

#### *Animal experiments of different HAp ceramics*

##### *Histological and immunochemical observations of explants*

The fg-HAp and rhBMP-2/fg-HAp ceramics were implanted into the subcutaneous tissues of the back region in 4-week-old male Wistar rats<sup>78,80-83)</sup>. At 4, 8, and 12 weeks after implantation, these samples were explanted. The specimens were fixed in neutral buffered formalin, decalcified with formic acid, embedded in paraffin, sectioned and stained with hematoxylin and eosin (HE).

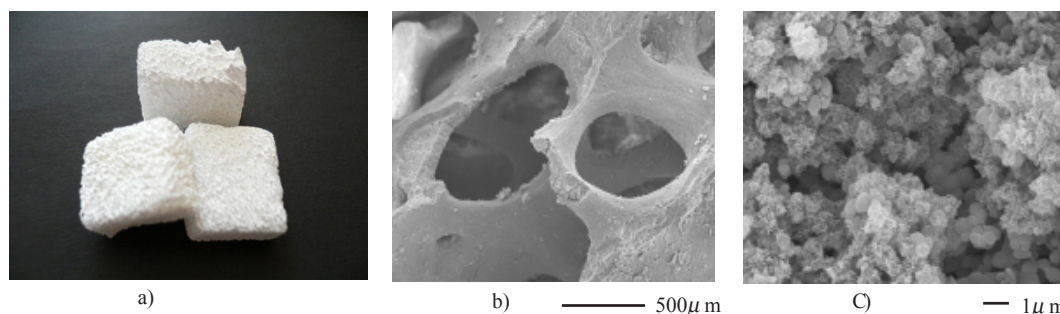


Figure 13 Appearance and SEM photographs of fg-HAp ceramics

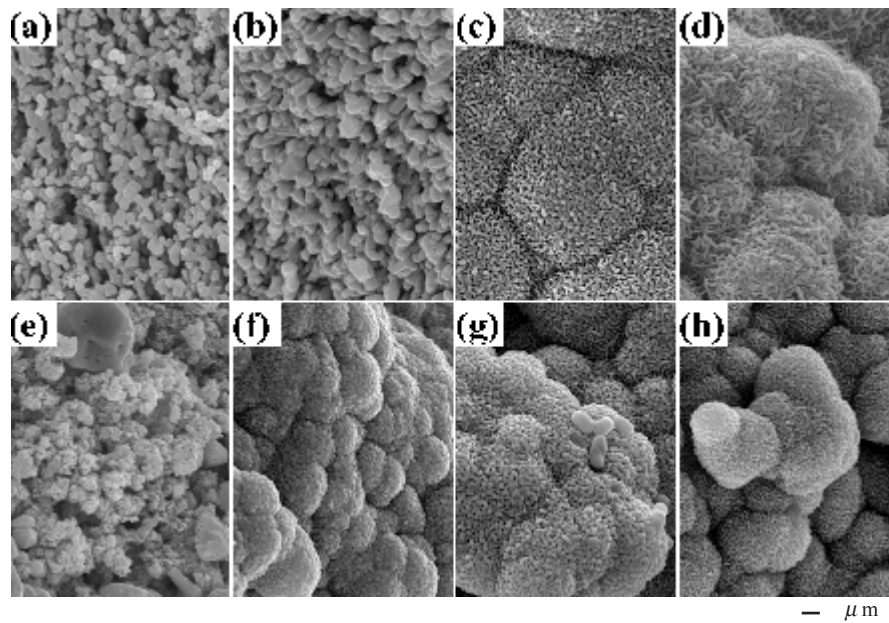


Figure 14. SEM photographs of f-HAp and b-HAp ceramics soaked at 36.5°C and pH 7.4 in SBF

They were histologically evaluated using an optical microscope. To investigate the eosinophilic areas in HE sections of the implanted ceramics, the specimens were immunostained with polyclonal rabbit antibody against rat albumin using the avidin-biotin complex method.

For the fg-HAp ceramics, at 4 weeks after the implantation, body fluid extensively permeated into the bulk regions of HAp through the nano-micro-pores of the ceramics<sup>80-84</sup>. In the macropores, many multinucleated giant cell and fibroblast were observed. Surface- and bulk- degradations of the HAp proceeded, so that a total size of the HAp block remarkably decreased. In the eosinophilic region of HE sections marked in the ceramics, the immunohistochemical staining was carried out. The immunostaining of albumin in the fg-HAp explant indicated to be immunopositive.

Figure 15 shows photographs of HE sections at 4 weeks after the implantation of rhBMP-2/fg-HAp ceramics. As a whole, geometrical relation of bone-HAp was like a mosaic image. Multinucleated giant cell on the crinkle HAp surface, HAp encapsulated in new bone, and retention of body fluid in HAp observed. The HAp fragmented by body fluid permeation and new bone formation from surface and bulk regions of the ceramics were observed. The HAp, which had been cut into small pieces, was incorporated into the induced bone, suggesting that osteoinduction occurred with bone remodeling<sup>77,81,83</sup>.

#### ***In vivo-release characteristics of rhBMP-2 from different HAp ceramics***

The <sup>125</sup>I-labeled rhBMP-2 (0.5μg) supported fg-HAp or b-HAp ceramics were implanted into the back subcutis of 6 week-age

female ddY mice. At 1-28 day after the implantation, the mice were sacrificed. The radioactivity of the remaining HAp ceramics, excised skin, and filter paper was measured on a gamma counter. Figure 16 shows changes in the retention percentage of rhBMP-2 for rhBMP-2/fg-HAp or b-HAp ceramics<sup>85</sup>. The retention percentages of rhBMP-2 decreased with increasing implantation

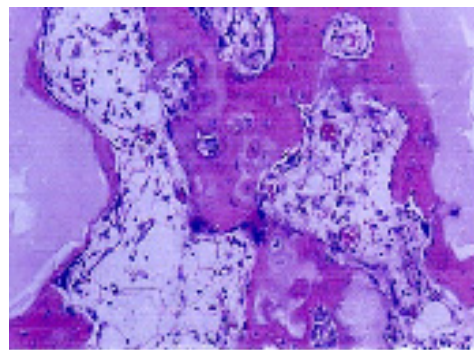


Fig. 15 shows a photomicrograph of histological sections at 4 weeks after the implantation of rhBMP-2/ fg-HAp ceramics

time. At 1-28 days after the implantation, the retention percentages of rhBMP-2 for fg-HAp are higher than those for b-HAp. Even at 14 days, the value for fg-HAp was about 60%, suggesting that fg-HAp ceramics are excellent osteoinductive scaffold. The difference in rhBMP-2-release between fg-HAp and b-HAp can be caused by differences in pore structure or adsorption strength of rhBMP-2 molecules on the HAp surfaces.

#### ***Expectation and a big prospect of regenerative therapy-studies in Hokkaido***

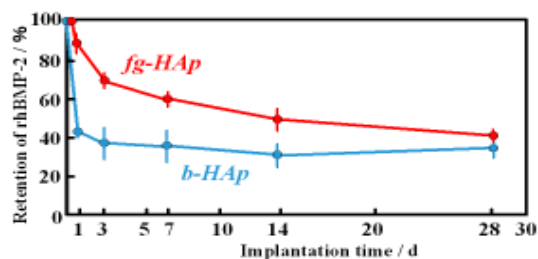


Figure 16. Changes in the retention percentage of rhBMP-2 for different HAp ceramics

The fg-HAp ceramics have excellent rhBMP-2-adsorption and release characteristics, as well as degradation-absorption due to body fluid permeation and blood permeability. The crystallinity and the pore size distribution of nano-particles can be designed and controlled by the calcination and partial dissolution-precipitation method. Since it was clarified that the rhBMP-2/fg-HAp was one of osteoinductive and bioabsorbable bioceramics related to bone-remodeling system, (Japanese patent No.3718723) was purchased in 2006<sup>77</sup>). Also, the fg-HAp ceramics might be applied for higher advanced medical care by strong connection with medical and dental teams. Hereafter, aiming for development and clinical application of artificial bone launching from Hokkaido into world, we are going to strengthen the alliance with the Department of Orthopedic Surgery, Graduate School of Medicine, Hokkaido University in the medical field and the Department of Oral Surgery, School of Dentistry, Health Sciences University of Hokkaido in the dental field. We would like to contribute acceleration of studies on biomaterials and development of medical industry, scoping *in vivo*-experiments for large animals and heightening the value of commercial biomaterials. Moreover, to improve many cases in Hokkaido and practice regenerative therapy for patients, interdisciplinary day-to-day collaboration prompting towards needs of medical locus, human network among the medical university and college in Hokkaido, establishment of Regeneration Therapy Center constituted by interdisciplinary project teams will be aspired.

##### 5) Dentin Matrices as a New Autograft Material for Osseous Regeneration

In this section, the animal and human-derived dentin research and a clinical pioneering case of autogenous demineralized dentin matrices transplant are described. The bone-inducing property of rabbit dentin matrices was discovered in 1967. We confirmed that completely demineralized dentin matrices (DDM) including small patches of cementum, derived from human adult extracted teeth, induced bone and cartilage independently in subcutaneous tissues at 4 weeks after implantation, while the calcified dentin matrices (CDM) did not induce hard tissues. In one study, a 22-year-old female with a congenital missing tooth of the mandibular right second premolar (#45) and an atrophied bone received tooth

autotransplantation with the freeze-dried DDM autograft. The patient's occlusion was successfully restored with the newly-developed biorecycle therapy using autogenous extracted teeth. Human DDM particles from a vital tooth have chondro-osteoinductive collagenous matrices, and autogenous DDM can be recycled as an autogenous biomaterial for bone regeneration. Human DDM particles can be recycled as an x biomaterial for bone regeneration.

##### Dentin and bone

Mineral crystals are deposited in extracellular organic substances during the development of bone and dentin. While the tissue structures of bone and dentin are different, the ratio of components is similar (mineral: about 70%, organic matrix: about 20%, liquid: about 10% by weight). Almost 90% of the organic matrix in dentin and bone consists of type I collagen, the remainder is non-collagenous proteins such as bone morphogenetic proteins (BMPs) and osteocalcin, and proteoglycan. Bone contains cellular components (osteocytes) and blood vessels. However, dentin is an acellular, avascular calcified matrix.

##### Bone induction by demineralized dentin

The history of a bone-inducing research in dentin began with a report in 1967 that rabbit demineralized dentin matrices (DDM) induced bone formation in the rabbit intramuscular pockets<sup>86</sup>. Until now, several dentin research papers have reported a chondro-osteoinductive potency of DDM and a BMP-like molecule in dentin matrices<sup>86-98</sup>. We confirmed that completely demineralized dentin particles derived from human adult extracted teeth, induced bone and cartilage independently in subcutaneous tissues of nude mice at 4 weeks after implantation<sup>98</sup>.

##### Basic studies of human dentin: Preparation of human demineralized dentin and non-demineralized dentin

Adult human third molar teeth were donated by outpatients at Health Sciences University of Hokkaido. The extracted third molar teeth were collected and prepared for completely demineralized dentin matrix (DDM) and non-demineralized dentin matrix, so called calcified dentin matrix (CDM). Briefly, the teeth were crushed in liquid nitrogen, washed in 1M sodium chloride, defatted with methanol/chlorophorum solution and rewashed for CDM. The CDM were demineralized completely in HCl solution (pH2.0) for DDM. The CDM and DDM particles were extensively rinsed in cold distilled water and lyophilized (Figures 17-19). The particle sizes varied from 0.4 to 0.8 mm.

##### Assay for biological activity and results

Seventy mg of DDM or CDM were put into cut-opened tuberculin syringes. Ten nude mice (male, 4 week-old, body weight; 50 g) were subjected to intraperitoneal anesthesia with pentobarbital sodium. A vertical incision (1 cm) was made under

sterile conditions in the skin over the back region, and 2 subcutaneous pockets were prepared by blunt dissection. Each animal received one DDM implant and one CDM implant. The implanted materials were removed at 4 weeks, and were prepared

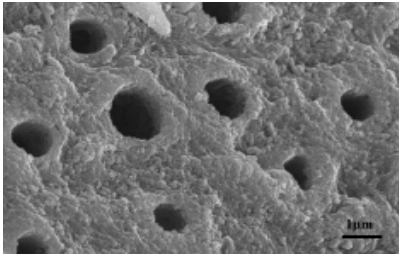


Figure 17. SEM of human calcified dentin matrix (CDM)

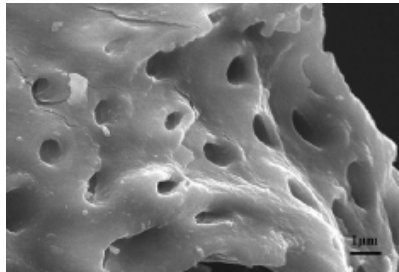


Figure 18. SEM of human demineralized dentin matrix (DDM) use



Figure 19. Freeze-dried human DDM particles before clinical

for histological observations. All procedures were followed the Guidelines in Health Sciences University of Hokkaido for Experiments on Animals.

DDM induced bone and cartilage, independently. New bone with osteoblast lining, not osteodentin, was found directly on the surface of DDM, while CDM did not induce hard tissue formation at 4 weeks (Figure 20).

#### ***Osteo-odonto-keratoprosthesis surgery using autologous dentin-bone***

A 49-year-old female lost her eyesight in end-stage Stevens-Johnson syndrome. A surprising operation for recovering the patient's eyesight, osteo-odonto-keratoprosthesis (OOKP) surgery was first done in 2003, Japan. The OOKP procedure utilizes an autologous tooth-bone complex to mount a polymethylmethacrylate optical cylinder as an artificial cornea. The root-bone complex and the plastic lens were fixed by dental adhesive cement, and the unit was stabilized by an overlying

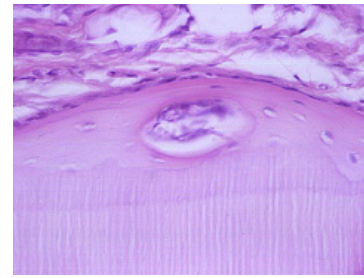


Figure 20. Induced bone on human DDM at 4 weeks

autologous buccal mucosal graft<sup>99</sup>). The patient's eyesight was restored to 1.0 vision through the OOKP surgery.

#### ***Dentin autograft into atrophied jaw for tooth autotransplantation***

A 22-year-old woman with reversed occlusion presented with a congenital missing tooth of the mandibular right second premolar (#45) and an atrophied bone. The medical history was essentially within normal limits and noncontributory. The quantity and quality of the atrophied bone and the length of teeth were estimated by CT scan. Upper premolar teeth (#14,#24) were extracted under the orthodontic planning. The vital tooth (#14) without root canal treatment was selected and prepared for freeze-dried DDM. Microdont (#28) which root was single (root length: 10mm, long



Figure 21. Immediate tooth autotransplantation simultaneously with DDM autograft



Figure 22. Reconstituted occlusion at 40 months after operation

width: 6mm) was chosen as transplanted tooth. The autogenous, immediate tooth transplantation with the freeze-dried DDM autograft was carried out in 2004 under the local anesthesia. Transplant cavity was formed using Flialit-2® dental implant system. As a limited osseous defect existed adjacent to the transplanted tooth, the defect was filled with particles of DDM, and bone augmentation on the perforated cortical bone was done by DDM (Figure 21). The mucoperiosteal flap was repositioned

and sutured. The patient was given an antibiotic for 3 days and getting on satisfactorily with no complications. Radiographic examination for the transplanted tooth area revealed a normal periodontal ligament space and an alveolar hard line at 40 months after the operation. The patient's occlusion was successfully reconstructed with the autograft of non-functional tooth and DDM (Figure 22).

The content of this paper has been described in detail to "Regenerative medicines of the bone and teeth"<sup>7100</sup>. Refer to this book for details.

#### Acknowledgment

The authors thank Professor DM Carlson, Matsumoto Dental University, for his critical reading of the manuscript.

#### References

1. Kuboki Y, Jin Q and Takita H. Geometry of carriers controlling phenotype expression in BMP-induced osteogenesis and chondrogenesis. *J Bone Joint Surg* 83-A: 105-114, 2001
2. Kuboki Y, Takita H, Mizuno M and Fujisawa R. Geometry of artificial extracellular matrices: a new paradigm from dental tissue engineering. *Dentistry Jpn* 37: 42-50, 2001
3. Jin Q-M, Takita H, Kohgo H, Atsumi K, Itoh H and Kuboki Y. Effects of geometry of hydroxyapatite as a cell substratum. *J Biomed Mater Res* 51: 491-199, 2000
4. Kuboki Y, Jin Q, Kikuchi M, Takita H. Geometry of artificial ECM: sizes of pores controlling phenotype expression in BMP-induced osteogenesis and chondrogenesis. *Connect Tissue Res* 43: 529-534, 2002
5. Mahmood J, Takita H, Kobayashi M, Kohgo T and Kuboki Y. Geometric effect of matrix upon cell differentiation: BMP-induced osteogenesis using a new bioglass with a feasible structure. *J Biochem* 129: 163-171, 2001
6. Urist MR. Bone formation by autoinduction. *Science* 150: 893-899, 1965
7. Reddi AH. Cell biology and biochemistry of endochondral bone development. *Collagen Rel Res* 1: 209-226, 1981
8. Wozney JM, Rosen V, Celeste AJ, Mitsock LM, Whitters MJ, Kriz RW, Hewick RM and Wang EA. Novel regulators of bone formation: molecular clones and activities. *Science* 242: 1528-1534, 1988
9. Rosen V. BMP and BMP Inhibitors in Bone. *Ann N Y Acad Sci* Apr 1068: 19-25, 2006
10. Kuboki Y, Saito T, Murata M, Takita H, Mizuno M, Inoue M, Nagai N and Poole AR. Geometrical factors of matrices for cell-differentiation. *Connect Tissue Res* 32: 219-226, 1995
11. Itoh H, Wakisaka Y, Ohunuma Y and Kuboki Y. A new porous hydroxyapatite ceramic prepared by cold isostatic pressing and sintering synthesized flaky powder. *Dent Mater J* 13: 25-65, 1994
12. Kuboki Y, Sasaki M, Saito A, Takita H and Kato H. Regeneration of periodontal ligament and cementum by BMP-applied tissue engineering. *Eur J Oral Sci* 106 (Suppl. 1): 197-203, 1998
13. Kuboki Y, Takita H, Kobayashi D, Tsuruga E, Inoue M, Murata M, Nagai N, Dohi Y and Ohgushi H. BMP-induced osteogenesis on the surface of hydroxyapatite with geometrically feasible and nonfeasible structures: topology of osteogenesis. *J Biomed Mater Res* 39: 190-199, 1998
14. Sasano Y, Ohtani E, Narita K, Kagayama M, Murata M, Saito T, Shigenobu K, Takita H, Mizuno, M and Kuboki Y. BMPs induce direct bone formation in ectopic sites independent of the endochondral ossification in vitro. *Anat Rec* 236: 373-380, 1993
15. Sasano Y, Mizuguchi I, Takahashi I, Kagayama M, Saito T and Kuboki Y. BMPs induce endochondral ossification in rats when implanted ectopically within a carrier made of fibrous glass membrane. *Anat Rec*. 247: 472-478, 1997
16. Tsuruga E, Takita H, Itoh H, Wakisaka Y and Kuboki Y. Pore size of porous hydroxyapatite as the cell-substratum controls BMP-induced osteogenesis. *J Biochem* 121: 317-324, 1997
17. Kuboki Y, Kikuchi M, Takita H, Yoshimoto R, Nakayama Y, Matsuda T, Ikada Y. Laser-perforated membranous biomaterials induced pore size-dependent bone induction when used as a new BMP carrier. *Connect Tissue Res* 44: 318-325, 2003
18. Kobayashi D, Takita H, Mizuno M, Totsuka Y and Kuboki Y. Time-dependent expression of bone sialoprotein fragments in osteogenesis induced by bone morphogenetic protein. *J Biochem (Tokyo)* 119: 475-481, 1996
19. Murata M, Inoue M, Arisue M, Kuboki Y and Nagai N. Carrier-dependency of cellular differentiation induced by bone morphogenetic protein in ectopic sites. *Int J Oral Maxillofac Surg* 27: 391-396, 1998
20. Kikuchi M, Takita H, Nakayama Y, Matsuda T and Kuboki Y. *J Hard Tissue Biol* 9: 79, 2000
21. Ito H, Aso Y, Furuse M, Noishiki Y and Miyata T. A honeycomb collagen carrier for cell culture as a tissue engineering scaffold. *Artif Org* 25: 213-217, 2001
22. Kuboki Y, Kaku T, Yoshimoto R, Kato K, Nemoto S, Iku M, Kono T, Miyata H, Takita H, Dong L and Kokai Y. 2004, Presented at 5th International Conference of BMP at Nagoya, September 12-16, 2004
23. Mizuno M, Kasagi T and Kuboki Y. Cross-linked collagen gel shares as a useful carrier for cell culture of MC3T3-E1 clonal osteogenic cells. *Jpn J Oral Biol* 30: 855-863, 1988
24. Kuboki Y, Yamaguchi H, Yokoyama A, Murata M, Takita H, Tazaki M, Mizuno M, Hasegawa T, Iida S, Shigenobu K,



- Fujisawa R, Kawamura M, Atsuta T, Matsumoto A, Kato H, Zhou H-Y, Ono I, Takeshita N and Nagai N. The Bone-Biomaterial Interface, J. D. Davies (Ed) Univ. Toronto Press, Toronto, p127. 1991
25. Takita H, Tsuruga E, Ono I and Kuboki Y. Enhancement by bFGF of osteogenesis induced by rhBMP-2 in rats. *Eur J Oral Sci* 105: 588-592, 1997
26. Kuboki Y, Takita H, Tsuruga E, Ono, M and Jansen JA. Rationale for hydroxyapatite-coated titanium-mesh as an effective carrier for BMP. *J Dent Res* 77 (Spec. A): 263, 1998
27. Vehof JW, Mahmood J, Takita H, Hof MA, Kuboki Y, Spauwen PHM, Jansen JA. Ectopic bone formation in titanium mesh loaded with bone morphogenetic protein and coated with calcium phosphate. *Plast Reconstr Surg* 108: 434-443, 2001
28. Kuboki Y, Yoshimoto R, Kato H, Dong L, Kaku T, Tanaka N, Kaneko M, Yanagisawa A, Tsuru T, Osaka A, Shiota H, Seki Y and Takita H. New paradigm of titanium-bone bonding: creation of the collaboration zone between the both substances, by use of 3-D titanium web, which is attached to the titanium bulk by vacuum sintering. *Arch Biocer Res* 5: 146-149, 2005
29. Reddi AH and Huggins CB. Influence of geometry of transplanted tooth and bone on transformation of fibroblast. *Proc Soc Exp Biol Med* 143: 634-637, 1973
30. Bassett C and Herrmann I. Influence of oxygen concentration and mechanical factors on differentiation of connective tissues in vitro. *Nature* 190: 460-461, 1961
31. Folkman J and Greenspan HP. Influence of geometry on control of cell growth. *Biochim Biophys Acta* 417: 211-236, 1975
32. Yoshimoto R, Takita H, Nemoto K and Kuboki Y. Attempt to arrest the cartilage stage in endochondral ossification by geometrical devices of an artificial ECM. *Arch Bioceramics Res* 5: 404-407, 2005
33. Nawata M, Wakitani S, Nakaya H, Tanigami A, Seki T, Nakamura Y, Saito N, Sano K, Hidaka E and Takaoka K. Use of bone morphogenetic protein 2 and diffusion chambers to engineer cartilage tissue for repair of defects in articular cartilage. *Arthritis Rheum* 52: 155-163, 2005
34. Reddi AH. *Advances in Biological and Medical Physics*, Lawrence, J. H. and Gofman, J. W., (eds.), Academic Press, New York, 1974
35. Yabu H and Shimomura M. Mesoscale pincushions, microrings, and microdots prepared by heating and peeling of self-organized honeycomb-patterned films deposited on a solid substrate. *Langmuir* 23: 4992-4997, 2006
36. Tsuruma A, Tanaka M, Fukushima N and Shimomura M. *E-Journal Surface Sci Nanotec* 3: 159, 2005
37. Ripamonti U, Crooks J and Kirkbride AN. Sintered porous hydroxyapatites with intrinsic osteoinductive activity: Geometric induction of bone formation. *South Afr J Sci* 95: 335-343, 1999
38. Kikuchi H, Kikuchi Y and Kuboki Y. Presented at the 3rd annual meeting of Japanese Tissue Engineering Society, Hiroshima, 2000
39. den Braber ET, de Ruijter JE, Ginsel LA, von Rectum AF and Jansen JA. Orientation of ECM protein deposition, fibroblast cytoskeleton, and attachment complex components on silicone microgrooved surfaces. *J Biomed Mater Res* 40: 291-300, 1998
40. Hirao M, Sugamoto K, Tamai N, Ika K, Yoshikawa H, Mori Y and Sasaki T. Macro-structural effect of metal surfaces treated using computer-assisted yttrium-aluminum-garnet laser scanning on bone-implant fixation. *J Biomed Mater Res A* 73: 213-222, 2005
41. Kondo N, Ogose A, Tokunaga K, Umezu H, Arai K, Kudo N, Hoshino M, Inoue H, Irie H, Kuroda K, Mira H and Endo N. Osteoinduction with highly purified beta-tricalcium phosphate in dog dorsal muscles and the proliferation of osteoclasts before heterotopic bone formation. *Biomater* 27: 4419-4427, 2006
42. Dong L, Iku S, Nemoto N, Kokai Y, Odajima T, Yoshimoto R, Kaku T, Katoh H, Shiota H, Seki Y, Ogura N, Abiko Y and Kuboki Y. *J Hard Tiss Biol* 14: 333, 2005
43. Weaver VW, Petersen OW, Wang F, Larabell CA, Briand P, Damsky C and Bissell MJ. Reversion of malignant phenotype of human breast cells in three dimensional culture and in vivo by integrin blocking antibodies. *J Cell Biol* 137: 231-245, 1997
44. Jacks T and Weinberg RA. Taking the study of cancer cell survival to a new dimension. *Cell* 111: 923-925, 2002
45. Ohgushi H, Goldberg VM and Caplan AI. *J Orthop Res* 7: 568, 1989
46. Ohgushi H, Y.Dohi, S.Tamai and S.Tabata. *J Biomed Mater Res*: 27: 1401, 1993
47. Yoshikawa T, Ohgushi H, Uemura H, Nakajima H, Ichijima K, and Samai T. *Biomed Mater Eng*: 8: 311, 1998
48. Ohgushi H, Kitamura S, Kotobuki N, Hirose M, Machida H, Muraki K and Takakura Y. *Yonsei Med J*. 45: S61, 2004
49. Suda T and Ozawa and Takahashi H.. *Science of Bone (Hone-no-Kagaku)*, Ishiyaku-Shuppan, Tokyo,129, 1985
50. Itoh S, M.ikuchi K, Takakuda K, Nagaoka K, Koyama Y, Tanaka J and Shinomiya K. *J Biomed Mater Res* 63: 507, 2002
51. Kikuchi M, Matsumoto HN, Yamada T, Koyama Y, Takakuda K and Tanaka J *Biomater*. 25: 63, 2004.
52. Itoh S, Kikuchi M, Koyama Y, Takakuda K, Shinomiya K and Tanaka J *Cell Transplant* 13: 451, 2004
53. Sotome S, Uemura T, Kikuchi M, Jiani C, Itoh S, Tanaka J and Shinomiya K, *Mater Sci Eng C* 24: 341, 2004

54. Hamberger V. The history of the discovery of the nerve growth factor. *J Neurol.* 24: 893-897, 1993
55. Cohen S. Isolation of a mouse submaxillary gland protein acceleration incisor eruption and eyelid opening in the newborn animal. *J Biol Chem* 237: 1555-1562, 1962
56. Gospodarowicz D. Localization of fibroblast growth factor and its effect alone and with hydrocortisone on 3T3 cell growth. *Nature* 249: 123-127, 1974
57. Bohlen P, Baird A, Esch F, Ling N, and Gospodarowicz D. Isolation and partial molecular characterization of pituitary fibroblast growth factor. *Proc Natl Acad Sci USA* 81: 5364-5368, 1984
58. Gimenez-Gallego G, Rodkey J, Bennett C, Rios-Candelore M, DiSalvo J and Thomas K. Brain-derived acidic fibroblast growth factor: complete amino acid sequence and homologies. *Science* 230: 1385-1388, 1985.
59. Nakamura T, Nawa K and Ichihara A. Partial purification and characterization of hepatocyte growth factor from serum of hepatectomized rats. *Biochem Biophys Res Commun* 122: 1450-1459, 1984
60. Ferrara N and Henzel WJ. Pituitary follicular cells secrete a novel heparin-binding growth factor specific for vascular endothelial cells. *Biochem Biophys Res Commun* 161:851-858, 1989
61. Leung DW, Cachianes G, Kuang WJ, Goeddel DV and Ferrara N. Vascular endothelial growth factor is a secreted angiogenic mitogen. *Science* 246: 1306-1309, 1989
62. Abraham JA, Whang JL, Tumolo A, Mergia A, Friedman J, Gospodarowicz D and Fiddes JC. Human basic fibroblast growth factor: nucleotide sequence and genomic organization. *EMBO J* 5: 2523-2528, 1986
63. Yuge T, Furukawa A, Nakamura K, Nagashima Y, Shinozaki K, Nakamura T and Kimura R. Metabolism of the intravenously administered recombinant human basic fibroblast growth factor, trafermin, in liver and kidney: degradation implicated in its selective localization to the fenestrated type microvasculatures. *Biol Pharm Bull* 20: 786-793, 1997
64. Cohen AM, Soderberg C and Thomason A. Plasma clearance and tissue distribution of recombinant human platelet-derived growth factor (B-chain homodimer) in rats. *J Surg Res* 49: 447-452, 1990
65. Nakamura T, Maruyama K, Sugimoto H, Nakamura M, Shibayashi T, Itoh A, Ikai M, Hashimoto K, Nakano Y, Yoshida M, Saito K and Kudo M. Three-month subcutaneous toxicity study of recombinant human basic fibroblast growth factor (KCB-1) in rats with and without one-month recovery study. *Iyakuhin-kenkyu* 27: 438-466, 1996
66. Bogousslavsky J, Victor SJ, Salinas EO, Pallay A, Donnan GA, Fieschi C, Kaste M, Orgogozo JM, Chamorro A and Desmet A. European-Australian fiblast (Trafermin) in acute stroke group: Fiblast (Trafermin) in acute stroke: results of the European-Australian phase I/II safety and efficacy trial. *Cerebrovasc Dis* 14: 239-251, 2002
67. Cooper LT Jr, Hiatt WR, Creager MA, Regensteiner JG, Casscells W, Isner JM, Cooke JP and Hirsch AT: Proteinuria in a placebo-controlled study of basic fibroblast growth factor for intermittent claudication. *Vascular Medicine* 6: 235-239, 2001
68. Nakamura K, Yuge T, Furukawa A, Nagashima Y, Kuwata Y, Uda K, Haino M and Awaji T: Distribution profiles of recombinant human basic fibroblast growth factor, KCB-1 in rats. *Kiso to Rinsho* 30: 1591-1603, 1996
69. Akazawa T. Production technology of cattle bone-originated apatites. *J High Temp Soc* 29 (3): 103-110, 2003
70. Aizawa M, Kanzawa N and Matsumoto M. Nano-structure of apatite-fiber scaffolds and its cell differentiation, *Biomater J Jpn Soc Biomater* 23 (5): 336-342, 2005
71. Murata M, Inoue M, Arisue M, Kuboki Y and Nagai N. Carrier-dependency of cellular differentiation induced by bone morphogenetic protein in ectopic site. *Int J Oral Maxillofac Surg* 27: 391-396, 1998
72. Murata M, Huang BZ, Shibata T, Imai S, Nagai N and Arisue M. Bone augmentation by recombinant human BMP-2 and collagen on adult rat parietal bone. *Int J Oral Maxillofac Surg* 28: 232-237, 1999
73. Murata M, Maki F, Sato D, Shibata T and Arisue M. Bone augmentation by onlay implant using recombinant human BMP-2 and collagen on adult rat skull without periosteum. *Clin Oral Implants Res* 11: 289-295, 2000
74. Nakajima T. Hydroxyapatite ceramics for spinal reconstruction, *Biomaterial. J Jpn Soc Biomater* 24(6): 405-412, 2006
75. Irie H. Application of biodegradable ceramics for bone regeneration., *Ceramics Jpn* 40 (10): 835-838, 2005
76. Murata M, Akazawa T and Arisue M. Bone engineering - Biological materials and bone morphogenetic proteins - *Phosphorus Res Bul* 17: 51-58, 2004
77. Akazawa T, Murata M, Arisue M, Kanno T and Kobayashi M. Japanese Patent No. 3718723.
78. Akazawa T, Murata M, Sasaki T, Tazaki J, Kobayashi M, Kanno T, Nakamura K and Arisue M. Biodegradation and bioabsorption innovation of the functionally graded bovine-bone originated apatite with blood permeability, *J Biomed Mater Res* 76A (1): 44-51, 2006
79. Akazawa T, Murata M, Tazaki J, Nakamura K, Itabashi K, Kanno T and Kobayashi M. Surface structure design and characterization of bioabsorbable and functionally graded apatites originated from bovine bone, *Key Engineer Mater* 309-311: 1051-1054, 2006
80. Akazawa T, Murata M, Tazaki J, Nakamura K, Itabashi K, Kanno T and Kobayashi M. Characterization of

- biodegradation and bioabsorption of functionally graded apatites originated from bovine bon. Phosphorus Res Bull 19: 118-123, 2005
81. Akazawa T, M Murata, Sasaki T, Tazaki J, Kobayashi M, Kanno T, Itabashi K and Arisue M. Osteoinduction by functionally-graded apatites of bovine origin loaded with bone morphogenetic protein-2. *J Am Ceramic Soc* 88(12): 545-3548, 2005
  82. Akazawa T, Murata M and Tazaki J. Materials design and osteoinduction characteristics of biomimetic and functionally graded apatites. *J Hard Tissue Biol* 14: 73-75, 2005
  83. Murata M, Akazawa T, Sasaki T, Ito K, Tazaki J, Yamamoto M, Tabata Y and Arisue M. Blood permeability of a novel ceramic scaffold for BMP-2. *J Biomed Mater Res* 81B: 469-476, 2007
  84. Akazawa T, Murata M, Tazaki J, Nakamura K, Itabashi K, Kanno T and Kobayashi M. Adsorption characteristics of albumin on bioabsorbable and functionally graded apatites originated from bovine bone. *Arch BioCeramics Res* 5: 332-335, 2005
  85. Tazaki J, Akazawa T, Murata M, Yamamoto M, Tabata Y, Yoshimoto R and Arisue M. BMP-2 dose-response and release studies in functionally graded Hap. *Key Engineer Mater* 309-311: 965-968 2006
  86. Yeomans JD and Urist MR. Bone induction by decalcified dentin implanted into oral, osseous and muscle tissues. *Arch Oral Biol* 12: 999-1008, 1967
  87. Bang G and Urist MR. Bone induction in excavation chambers of decalcified dentin. *Arch Surg* 94:781-789, 1967
  88. Huggins C and Urist MR. Transplantation: Rapid induction of Alkaline phosphatase and cartilage. *Science* 167:896-897, 1970
  89. Huggins C, Wiseman S and Reddi AH. Transformation of fibroblasts by allogeneic and xenogeneic transplants of demineralized tooth and bone *J Exp Med.* 132: 1250-1258, 1970
  90. Butler WT, Mikulski A, Urist MR, Bridges G and Uyeno S. Noncollagenous proteins of a rat dentin matrix possessing bone morphogenetic activity. *J Dent Res* 56: 228-232, 1977
  91. Yahagi S. An experimental study on cartilage and morphogenesis induced by implantation of demineralized dentin matrix. *Shika Gakuh* 85: 135-165, 1985
  92. Inoue T, Deporter DA and Melcher AH. Induction of chondrogenesis in muscle, skin, bone marrow, and periodontal ligament by demineralized dentin and bone matrix *in vivo* and *in vitro*. *J Dent Res* 65: 12-22, 1986.
  93. Kawai T and Urist MR. Bovine tooth-derived bone morphogenetic protein. *J Dent Res* 68: 1069-1074, 1989
  94. Bessho K, Tagawa T and Murata M. Purification of rabbit bone morphogenetic protein derived from bone, dentin and wound tissue after tooth extraction. *J Oral Maxillofac Surg* 48:162-169, 1990
  95. Bessho K, Tanaka N, Matsumoto J, Tagawa T and Murata M. Human dentin-matrix-derived bone morphogenetic protein. *J Dent Res* 70: 171-175, 1991
  96. Iboki M. Experimental studies on induction of cartilage and bone by human dentin matrix. *Jpn J Oral Maxillofac Surg* 37: 1-14, 1991
  97. Nebgen DR, Inoue H, Sabsay B, Wei K, Ho C-S and Veis A. Identification of the chondrogenic-inducing activity from bovine dentin (bCIA) as a low-molecular-mass amelogenin polypeptide. *J Dent Res* 78: 1484-1494, 1999
  98. Murata M, Sato D, Akazawa T, Taira T, Sasaki T and Arisue M. Bone and cartilage induction in nude mice by human demineralized dentin matrix. *J Hard Tissue Biol* 11: 110-114, 2003
  99. Tay AB, Tan DT, Lye KW, Theng J, Parthasarathy A and Por YM. Osteo-odonto-keratoprosthesis surgery: a combined ocular-oral procedure for ocular blindness. *Int J Oral Maxillofac Surg* 36(9): 807-813, 2007
  100. Kawakami T and Kuboki Y ed. *Regenerative Medicine of Bone and Teeth, with special references to biological principles, problems and their indicators.* Gakusaikikaku Pub, Tokyo Japan pp 1-114, 2007